Scientific Reports

https://doi.org/10.1038/s41598-026-45598-8

Article in Press

Assessment of levels spatiotemporal differences and health risks of environmental radioactivity in the soil of Chongqing China

Received: 28 August 2025

Accepted: 20 March 2026

Published online: 25 March 2026

Cite this article as: Huang Q., Zhao X., Fang B. *et al.* Assessment of levels spatiotemporal differences and health risks of environmental radioactivity in the soil of Chongqing China. *Sci Rep* (2026). https://doi.org/10.1038/s41598-026-45598-8

Qiang Huang, Xue Zhao, Bo Fang, Qiang Tan, Qiuhao Zhang, Li Chen, Cuilan Fang, Hengyan Du & Jun Diao

Title: Assessment of levels spatiotemporal differences and health risks of environmental radioactivity in the soil of Chongqing China

Author: Qiang Huang[1,5], Xue Zhao[3,5], Bo Fang[2], Qiang Tan[1], Qiuhao Zhang[4], Li Chen[2], Cuilan Fang[2], Hengyan Du[4], Jun Diao[2*]

[1] Chongqing Center for Disease Control and Prevention, Chongqing, China.

[2]Chongqing Jiulongpo District Center for Disease Control and Prevention, Chongqing, China.

[3] Chongqing Radiation Environment Supervision and Management Station, Chongqing, China.

[4]School of Public Health, Chongqing Medical University, Chongqing, China.

[5] Qiang Huang and Chao Xue contributed equally to this study.

[*] Correspondence: Jun Diao, jundiaojundiao@163.com.

Abstract: This study investigated the spatio-temporal variations of soil radionuclides in Chongqing (2016-2023) and assessed their associated health risks. Using descriptive, correlation, and mixed-effects model analyses, the activity concentrations and distribution of soil radionuclides (^{137}Cs, ^{238}U, ^{232}Th, ^{226}Ra and ^{40}K) were examined. AEDE, Ra_{eq}, ELCR, ADR were calculated. Spatially, after controlling for temporal variation, the Urban New Area showed higher ^{226}Ra and ^{238}U than the Urban Core Area, while the Southeast Wuling Mountain Area had higher ^{226}Ra, ^{137}Cs and ^{238}U. Temporally, after controlling for regional variation, ^{40}K (2023, 2021), ^{232}Th (2018-2023) and ^{238}U (2021) all exhibited higher activity concentrations than in 2016. The calculated health risk indices (AEDE, Ra_{eq}, ELCR, ADR) were above global averages, indicating a need for targeted soil management. Specifically, levels of ^{226}Ra and ^{238}U in the Urban New Area, and of ^{226}Ra, ^{137}Cs, ^{232}Th and ^{238}U in the Southeast Wuling Mountain Area, require prioritization.

Keywords

Chongqing, soil radionuclides, spatio-temporal variations, health risks, radium equivalent, dose rate

Introduction

The origins, occurrence, and environmental distribution of radionuclides, ubiquitous in natural systems, are critical in shaping their impacts on ecological integrity and human health[1]. Primordial radionuclides can be classified into two groups: one comprising decay-series radionuclides formed by the three naturally occurring radioactive series (i.e., thorium, uranium, and actinium), and the other consisting of decay-series radionuclides derived from single-decay radionuclides such as potassium (K), rubidium (Rb), lanthanum (La), samarium (Sm), and lutetium (Lu)[2]. These have persisted throughout Earth's history and serve as the primary contributors to natural radioactivity. They are not only present within the soil of the lithosphere but also enter aquatic systems and the atmosphere via natural processes including groundwater circulation and weathering, thereby impacting the entire ecosystem[3]. Furthermore, with the increase in anthropogenic activities such as nuclear energy utilization, weapons testing, and nuclear accidents, artificial radionuclides have gradually become a non-negligible component of the environmental inventory. The generation of artificial radionuclides depends on nuclear reactions, including nuclear fission, nuclear fusion, particle bombardment and secondary reactions, with typical examples including ^{137}Cs, ^{90}Sr, ^{131}I, ^{3}H, ^{60}Co[4-6].

The migration rate of radionuclides within environmental media is subject to multiple factors, including their physicochemical properties, the characteristics of the environmental matrix, and prevailing environmental conditions[7]. The migration of radioactive nuclides through soil significantly

impacts ground-level gamma radiation levels[8]. Consequently, soil serves as one of the primary sources of radiation transfer into the environment. Radioactive nuclides in soil also comprise three categories. The first category consists of primordial radionuclides, with ^{40}K, ^{238}U, ^{232}Th and ^{226}Ra representing major contributors to natural radioactivity in soil and their radiological hazard primarily occurs through the emission of gamma rays and the inhalation of radon isotopes and their progeny[9]. The second type originates from nuclear tests and nuclear accidents. ^{137}Cs primarily enters the soil through precipitation and is subsequently redistributed mainly via the movement of soil and sediment particles[10, 11]. The last one comes from cosmogenic radionuclides (e.g., ^{7}Be, naturally occurring ^{3}H and ^{14}C), produced by cosmic ray interactions. However, its direct impact on soil is limited (such as slight change in radioactive balance and chemical environment). These radionuclides in the soil can affect human health both directly through contact and indirectly through the food chain. Studies have shown that the decay of ^{238}U releases alpha particles, and its inhalation or ingestion increases the risk of lung and bone cancers[12]. The alpha-emitting ^{226}Ra decays into radon gas isotopes (e.g., ^{222}Rn). Inhalation of these isotopes and their progeny is the second leading cause of lung cancer after smoking[13]. The decay of ^{232}Th emits alpha particles, and inhalation of its dust or ingestion via the food chain may elevate the risk of lung and pancreatic cancers[14]. ^{137}Cs can be absorbed by plants and transferred to humans through food products such as milk and meat, thereby increasing the risk of several cancers, including soft-tissue sarcomas and leukemia[15].

Chongqing Municipality is situated in the transitional zone between the Qinghai-Tibet Plateau and the middle-lower Yangtze Plain, characterized predominantly by mountainous and hilly terrain. By the end of 2023, 72 mineral resources had been identified in the region, with proven reserves for

46 species, including widespread distributions of natural gas and shale gas[16]. Additionally, Chongqing had long prioritized agricultural development and a substantial quantity of fertilizer was utilized, encompassing phosphate fertilizer, potash fertilizer, and compound fertilizer. Therefore, the baseline levels of radionuclides in Chongqing's soils may be primarily attributed to geological features, while acknowledging the potential influence of other factors such as fertilizer use. Those suggests that the local population may face elevated exposure to radionuclides through food chain pathways. Consequently, monitoring soil radionuclide levels is important for safeguarding public health. However, relevant studies in Chongqing remain scarce. To address this knowledge gap, this study systematically investigated soil samples collected from 28 districts and counties across Chongqing Municipality between 2016 and 2023. This study aim to understand the levels, regional and temporal differences of radioactive nuclides in soil of Chongqing from 2016 to 2023, assess their health risks to the people of Chongqing, and provide theoretical basis for the formulation and implementation of relevant laws and regulations in Chongqing.

Methods

Sample collection and testing

This study employed stratified random sampling, where the Urban Core Area was 100% included, while Urban New Area, Three Gorges Reservoir Area Urban Agglomeration in Northeast Chongqing and Wuling Mountain Area Urban Agglomeration in Southeast Chongqing were sampled at a rate of approximately 66%. Soil samples were collected from public areas in 28 districts and counties of Chongqing (Figure 1). These areas included public farmland, public green spaces, and buffer zones of natural reserves open to scientific research. For undisturbed soil samples, soil from the 0-5 cm depth was generally collected as the topsoil sample. For samples from

human-disturbed sampling sites (such as farmland), the soil above 30 cm was basically mixed due to human cultivation activities. Therefore, soil from the 0-30 cm depth from the ground was collected as the sample. Each year, the sampling points were located in areas with flat terrain, relatively no pollution (low population density in the vicinity of sampling points, absence of large industrial facilities, no landfills or incineration plants, and being situated away from airports and major highways), less gravel, thick soil layers, and no waterlogging and soil samples were collected from GPS-located fixed points. Depending on the terrain, a quincunx or serpentine pattern was employed to collect sub-samples from five locations, which were then homogenized to form a composite sample. Approximately 1 kg of sample was collected, placed in a plastic bag, and transported to the laboratory. Subsequently, stones and plant debris (e.g., weeds) were removed by sieving. The samples were then oven-dried at 105°C, ground using a ball mill, passed through a 60-mesh sieve, and stored in a cylindrical polyvinyl chloride sample container (with dimensions of 75 mm outer diameter, 70 mm outer height, 2.5 mm wall thickness, 2.5 mm bottom thickness, and a sample filling height of 65 mm), sealed for more than 20 days, and then analyzed by high-purity germanium gamma spectrometry. Finally, the activities of radionuclides ^{40}K, ^{137}Cs, ^{226}Ra, ^{232}Th and ^{238}U in soil samples were detected by C7080 high-purity germanium gamma spectrometer from Canberra, USA basing on "General Method for Gamma-ray Spectrometry with High-Purity Germanium Detectors" (GB/T 11713-2015) and "Method of Gamma-ray Spectrometry for Analysing Radionuclides in Environmental and Biological Samples" (GB/T 16145-2022). Internal quality control was ensured through the analysis of parallel and retained samples. Additionally, instrument performance was verified through regular calibration, long-term reliability assessments (utilizing background and efficiency quality control charts), and Poisson distribution tests. For instance, the measurement parameters for a sample mass of 275 g are provided as follows (Table 1 and Figure 2). The detector

energy calibration uses ^{241}Am, ^{137}Cs, ^{60}Co, ^{152}Eu, and the efficiency calculation uses certified reference materials with known active concentrations, obtained from the Shanghai Institute of Metrology and Testing Technology, China (reference number: 23E06042). Its geometry was identical to that of the measured samples, and the source contained all target radionuclides of interest. The energy resolution of the high-purity germanium detector is 1.89 keV and the gamma spectrometer was capable of detecting and displaying the characteristic energy peaks of all daughter gamma nuclides in the sample on the spectrum, whereas the primary characteristic energy peak with the highest weight was typically selected for quantitative calculation. Finally, the detection limit was calculated using the following formula.

$$LLD = \frac{2.83K}{\square \times \varepsilon_{p.\gamma}(E_r)}\sqrt{\frac{n_b}{T_b}}$$

n_b- The background count rate within the full-energy peak region of the characteristic gamma ray selected for the nuclide to be estimated

T_b-Background measurement time, in seconds (s)

$\varepsilon_{p.\gamma}(E_r)$-Full absorption peak detection efficiency of the gamma ray

$\square$-The emission probability of the selected characteristic gamma ray for the nuclide

K-This refers to the value of the probability of incorrectly judging that there is no radioactivity exceeding the LLD in the sample, when such radioactivity actually exists in the sample

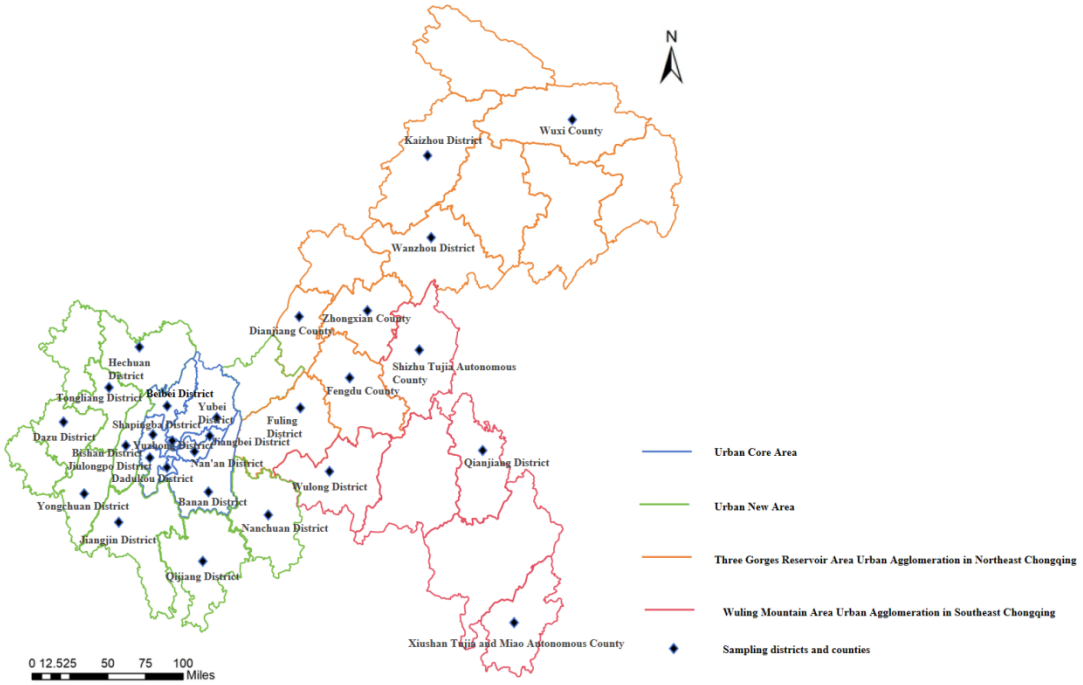

Figure1. Sampling point distribution map in Chongqing, China. The map was generated using R (version 4.4.2, https://www.r-project.org/). Administrative boundary data were obtained from the AliCloud DataV geographic data repository (https://geo.datav.aliyun.com/areas_v3/bound/500000_full.json)

Table 1. Parameters for instrument measurement

Target nuclides	Measured nuclides	Energy (keV)	Measurement time (h)	Detection efficiency (%)	Detection limit (Bq/kg)
^{40}K	^{40}K	1460.8	24	1.35	3.03
^{137}Cs	^{137}Cs	661.7	24	2.16	0.27
^{226}Ra	^{214}Pb	351.9	24	3.13	0.72
^{232}Th	^{228}Ac	911.2	24	1.78	0.83
^{238}U	^{234}Th	63.3	24	4.38	7.27

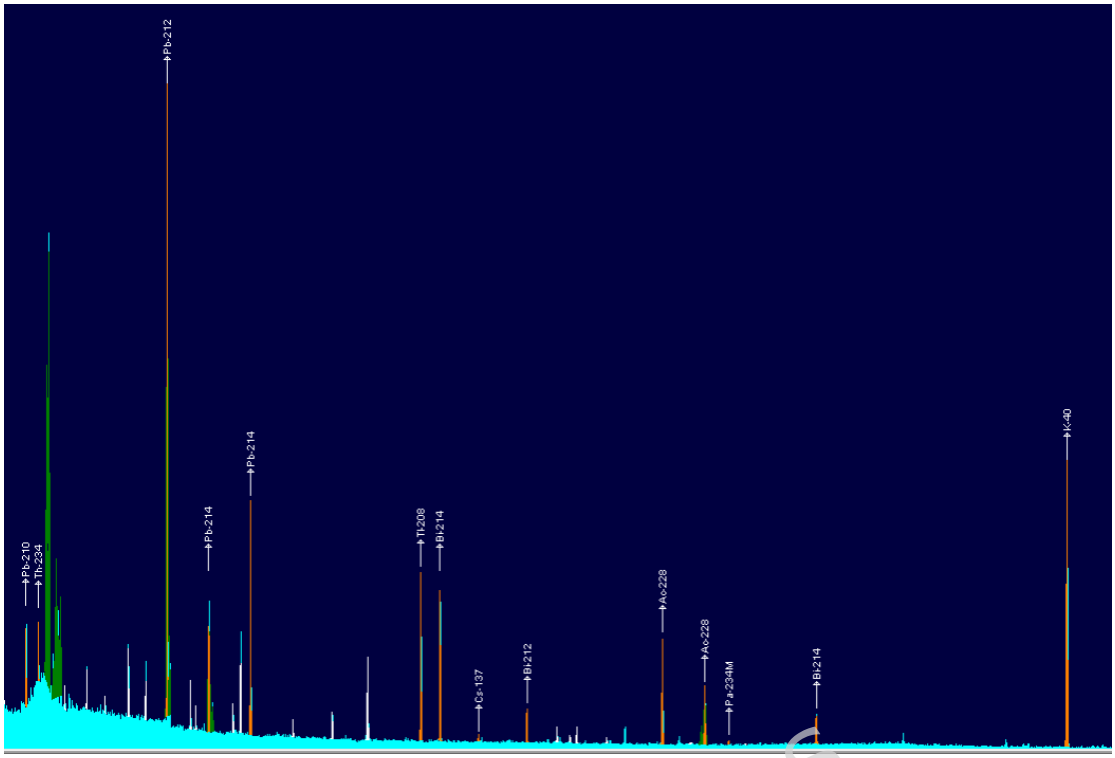

Figure2. Measured gamma-ray spectrum

Evaluation of the radiological health risk

The radium equivalent activity (Ra_{eq}) is a comprehensive index used to evaluate the gamma radiation hazard from soil containing multiple natural radionuclides (^{226}Ra, ^{232}Th and ^{40}K)[17]. It is calculated using a standardized formula that weights the activity concentrations of each radionuclide by its respective gamma-ray potency relative to ^{226}Ra. The contribution of ^{137}Cs was calculated (contribution rate below 0.5%) and found to be negligible in our samples compared to the primordial radionuclides.

$$\alpha(Ra_{eq}) = \alpha(^{226}Ra) + \alpha(^{232}Th) \times 1.43 + \alpha(^{40}K) \times 0.077$$

$\alpha(^{226}Ra)$- ^{226}Ra activity concentration ($Bq \cdot kg^{-1}$)

$\alpha(^{232}Th)$- ^{232}Th activity concentration ($Bq \cdot kg^{-1}$)

$\alpha(^{40}K)$- ^{40}K activity concentration ($Bq \cdot kg^{-1}$)

γ dose equivalent rate (ADR) is one of the core indicators to assess the risk of radiation exposure to public health. High dose rate means high radiation

exposure risk, and it is an important indicator of environmental radiation level[18].

$$ADR = \alpha(^{238}U)\times 0.462 + \alpha(^{232}Th)\times 0.604 + \alpha(^{40}K)\times 0.0417$$

ADR (nGy•h^{-1})

0.462 - ^{238}U nuclide dose coefficient (nGy•h^{-1} per Bq•kg^{-1}) [19]

0.604 - ^{232}Th series nuclide dose coefficient (nGy•h^{-1} per Bq•kg^{-1})[19]

0.0417 - ^{40}K dose coefficient (nGy•h^{-1} per Bq•kg^{-1})[19]

Annual effective dose equivalent rate (AEDE) is a key metric in radiation protection used to quantify the radiation dose received by a member of the public over one year due to chronic exposure to environmental radiation[20].

$$AEDE = ADR \times 8760 \times 0.2 \times 0.7 \times 10^{-3}$$

AEDE(μSv•a^{-1})

8760 - Time conversion factor

0.2 - Outdoor occupancy factor

0.7 - Dose conversion factor to convert absorbed dose to effective dose in air (Sv•Gy^{-1})

Excess Lifetime Cancer Risk (ELCR) is defined as the additional probability of an individual developing cancer due to exposure to carcinogens (such as radiation or chemicals) over their lifetime, beyond the baseline risk posed by natural background exposure[21]. This metric serves to quantify the contribution of specific exposures to the lifetime risk of cancer incidence.

$$ELCR = AEDE \times F \times L$$

ELCR (dimensionless).

F - Random effect risk factor (Sv^{-1}), which is 0.05 according to ICRP report[22]

L - Expected lifetime, taking 78.2 (years) according to the report of the

Chinese government[23]

Statistical analysis

This study collected the soil monitoring data of 28 districts and counties in Chongqing from 2016 to 2023, and analyzed the data using R version 4.4.2. Based on Chongqing's geographical location, economic development level, and historical-cultural connections, the municipality was categorized into four regions, namely the Urban Core Area (UCA), Urban New Area (UNA), Three Gorges Reservoir Area Urban Agglomeration in Northeast Chongqing (TGRA-UA-NE Chongqing), and Wuling Mountain Area Urban Agglomeration in Southeast Chongqing (WMA-UA-SE Chongqing). The regional classification of 28 districts and counties is shown in Table 2. In this study, the numerical data were described by mean ± standard deviation, and the differences of radionuclides in soil at different times and regions were analyzed by repeated measurement analysis of variance. Spearman correlation analysis was used to confirm the relationship among ^{40}K, ^{137}Cs, ^{226}Ra, ^{232}Th and ^{238}U. The mixed effects model is the core tool for processing dependent data in experimental design and it optimizes statistical inference by considering both fixed effects and random effects[24]. In this study, the year and region were taken as fixed effects and random effects, respectively, to clarify the differences of different radionuclides in soil in time and region. Model1 (regional differences model): radioactivity level ~ region + (1 | year) with "UCA" as the reference level and model2 (temporal trend model): radioactivity level ~ year + (1 | region) with "2016" as the reference level. In this study, principal component analysis (PCA) was used to analyze the principal components of radionuclides ^{40}K, ^{137}Cs, ^{226}Ra, ^{232}Th and ^{238}U and the related parameters Ra_{eq}, ADR, AEDE, ELCR. The correlation coefficient distance between radionuclide mass activity and other related indicators was calculated by cluster analysis.

Table 2. The regional classification of 28 districts and counties

Regions	N	n	District/county
UCA	9	9	Yuzhong District, Dadukou District, Jiangbei District, Shapingba District, Jiulongpo District, Nan'an District, Beibei District, Yubei District, Banan District
UNA	12	8	Jiangjin District, Hechuan District, Yongchuan District, Nanchuan District, Qijiang District, Dazu District, Bishan District, Tongliang District
TGRA-UA-NE Chongqing	11	7	Wanzhou District, Fuling District, Kaizhou District, Fengdu County, Dianjiang County, Zhongxian County and Wuxi County.
WMA-UA-SE Chongqing	6	4	Qianjiang District, Wulong District, Shizhu Tujia Autonomous County, Xiushan Tujia and Miao Autonomous County

N-The total number of regions

n-The number of extracted regions

Result

Characteristics of terrestrial radionulides in Chongqing from 2016 to 2023

The present study found that there were significant differences in ^{40}K (F=6.272, P<0.001), ^{232}Th (F=24.390, P<0.001), ^{238}U (F=3.424, P=0.002<0.05) over the eight years, as summarized in Table 3 and illustrated via line graphs in Figure 3. The results showed that there were statistically significant differences in the distribution of ^{137}Cs (F=10.45, P=0.001<0.05), ^{232}Th (F=4.745, P=0.031<0.05) and ^{238}U (F=8.112, P=0.005<0.05) in different regions, as shown in Table 4. A comparative analysis of activity concentrations of ^{238}U, ^{232}Th, ^{226}Ra and ^{40}K in soils

worldwide is shown in Table 5.

Table 3. Year-wise variation in activity concentrations of soil-related radionuclides in Chongqing during the period 2016-2023

Years	^{40}K (Bq•kg^{-1})	^{137}Cs (Bq•kg^{-1})	^{226}Ra (Bq•kg^{-1})	^{232}Th (Bq•kg^{-1})	^{238}U (Bq•kg^{-1})
2016	527±152	1.37±2.64	36.2±14.3	39.1±8.1	34.3±13.1
2017	533±130	1.21±2.44	35.9±13.4	40.0±7.1	36.7±10.1
2018	557±154	1.49±2.32	36.3±14.2	47.9±9.9	39.7±14.6
2019	575±99	1.01±0.96	32.8±13.5	44.6±8.0	40.0±14.9
2020	538±146	0.85±1.39	32.3±13.5	45.0±8.5	38.9±13.7
2021	668±155	0.80±0.35	39.7±15.3	54.7±7.8	42.2±16.3
2022	551±125	1.08±1.55	39.8±33.8	47.0±6.7	38.0±15.6
2023	605±123	0.86±0.68	40.1±43.0	48.6±7.4	39.7±19.7
F	6.272	1.088	1.709	24.390	3.424
P	<0.001	0.373	0.11	<0.001	0.002

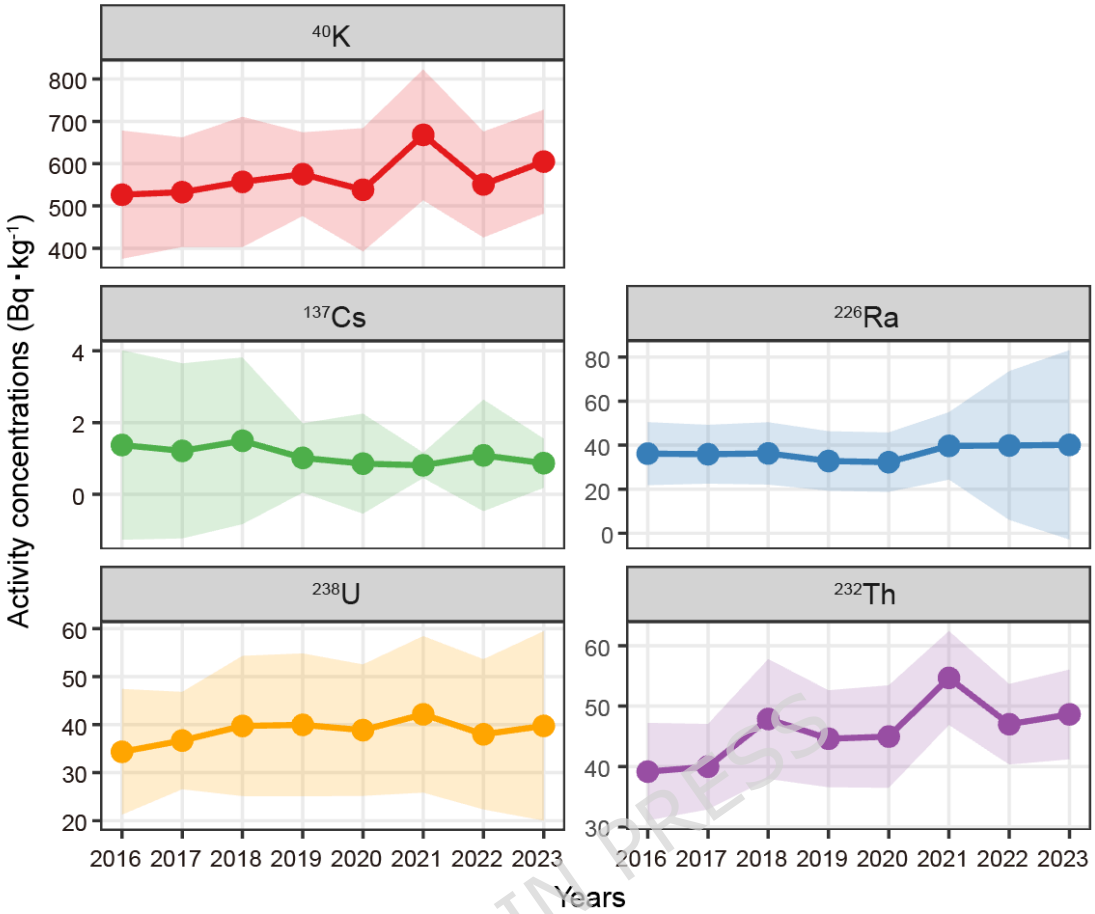

Figure 3. Variation of soil related radionuclide activity concentrations in Chongqing from 2016 to 2023

Table 4. Mean activity concentration of various radionuclides in Chongqing from 2016 to 2023

Regions	^{40}K (Bq•kg^{-1})	^{137}Cs (Bq•kg^{-1})	^{226}Ra (Bq•kg^{-1})	^{232}Th (Bq•kg^{-1})	^{238}U (Bq•kg^{-1})
UCA	582±98	0.78±0.60	31.1±7.2	45.1±7.7	34.6±7.1
UNA	545±151	0.82±0.69	45.4±40.1	47.0±7.6	43.2±21.1
TGRA-UA-NE					
Chongqing	618±130	1.19±1.60	31.6±12.6	43.3±8.9	34.8±14.2
WMA-UA-S	534±205	2.11±3.51	41.9±13.0	49.5±13.1	46.5±14.3

E Chongqing					
F	0.040	10.450	1.786	4.745	8.112
P	0.842	0.001	0.183	0.031	0.005

Table 5. Comparative analysis of activity concentrations of ^{238}U, ^{232}Th, ^{226}Ra and ^{40}K in soils from different regions of the world.

Locations	^{238}U (Bq•kg^{-1})	^{232}Th (Bq•kg^{-1})	^{226}Ra (Bq•kg^{-1})	^{40}K (Bq•kg^{-1})	^{137}Cs (Bq•kg^{-1})	References
Global median	16-110 (35)	11-64 (30)	17-60 (35)	140—850 (400)		UNSCEAR, 2008[19]
Population-weighted average	33	45	32	420		UNSCEAR, 2008[19]
Punjab, Pakistan		42-53 (47)	34-43 (39)	532-621 (569)		Faheem et al., 2008[25]
Kelantan, Malaysia			49-251 (145)	491-2496 (908)		Hamzah et al., 2012[26]
Turkey	2-220 (29)	1-159 (33)		26-1603 (449)	1-357 (13)	Turhan et al., 2012[27]
Azad Kashmir, Pakistan		28-73 (44)	13-60 (31)	250-896 (575)	2-69 (15)	Rafique et al., 2013[28]
West Bengal, India		7-22 (17)	24-34 (29)	461-610 (518)		Sharma et al., 2023[29]
Isparta, Turkey		3-66 (15)	4-69 (16)	44-452 (211)	0.3-19 (3)	Kürkçüoğlu et al., 2024[30]
Kano, Nigeria		50-122 (72)	41-102 (65)	253-1227 (681)		Muhammad et al., 2024[31]
Yemen		33-211	28-81	ND-1235		Maglas et al.,

						2024[32]
Phosphate	<0.1-43.5	5-56 (27)	103-529			Machraoui et al.,
Area, Tunisia	(13)		□264□			2024[33]
Chongqing,	17.6-137	18-73.9	17-275	102-1094	0.2-13.8	Our study
China	(39)	(46)	(37)	(571)	(1.1)	

The data are presented as minimum–maximum (mean) values. Not Detected (ND)

Correlation analysis of soil related radionuclides in Chongqing from 2016 to 2023

It was found that ^{232}Th showed significant positive correlations with both ^{40}K (r=0.455, P<0.01) and ^{226}Ra (r=0.543, P<0.01). Concurrently, ^{238}U exhibited a very strong significant positive correlation with ^{226}Ra (r=0.754, P<0.01), and was also significantly positively correlated with ^{232}Th (r=0.550, P<0.01) and ^{137}Cs (r=0.145, P<0.01). In contrast, ^{137}Cs was significantly negatively correlated with ^{40}K (r=-0.205, P<0.01). The correlations between ^{40}K and ^{226}Ra or ^{238}U, as well as between ^{137}Cs and ^{226}Ra or ^{232}Th, were not statistically significant (P>0.05), as shown in Table 6.

Table 6. Correlation analysis of soil related radionuclides in Chongqing from 2016 to 2023

Variables	^{40}K	^{226}Ra	^{137}Cs	^{232}Th	^{238}U
^{40}K	1				
^{226}Ra	0.094	1			
^{137}Cs	-0.205**	-0.030	1		
^{232}Th	0.455**	0.543**	0.039	1	
^{238}U	-0.017	0.754**	0.145*	0.550**	1

** P<0.01

* P<0.05

Analysis of temporal and regional differences of radionuclides in soil of Chongqing

The study found that after controlling the impact of time changes, the activity concentrations of ^{226}Ra and ^{238}U in UNA were 14.314 and 8.676 ($Bq \cdot kg^{-1}$) higher than those in UCA, respectively. The activity concentrations of ^{226}Ra, ^{137}Cs, ^{232}Th and ^{238}U in WMA-UA-SE Chongqing were 10.813, 1.334, 4.331 and 11.928 ($Bq \cdot kg^{-1}$) higher than those in UCA, respectively, with no significant difference in the rest. Model2 results showed that after controlling the influence of regional differences, the activity concentrations of ^{40}K in 2023 and 2021 were 77.61 and 140.98 ($Bq \cdot kg^{-1}$) higher than that in 2016, and the activity concentrations of ^{232}Th in 2018, 2019, 2020, 2021, 2022 and 2023 were 8.705, 5.565, 5.925, 15.637, 7.971 and 9.598 ($Bq \cdot kg^{-1}$) higher than that in 2016, and the ^{238}U in 2021 was 7.765 ($Bq \cdot kg^{-1}$) higher than that in 2016. Other differences were not statistically significant. Those results were displayed in Table 7.

Table 7. Temporal and regional differences of radionuclides in soil of Chongqing with respect to control parameters of Model1 and Model2

Variables	^{40}K		^{226}Ra		^{137}Cs		^{232}Th		^{238}U	
	Estimate	*P*	Estimate	*P*	Estimate	*P*	Estimate	*P*	Estimate	*P*
Model1										
UNA	-38	0.071	14.3	<0.001	0.04	0.88	1.6	0.195	8.7	<0.001
TGRA-UA-NE	33	0.18	0.5	0.903	0.41	0.171	-2.3	0.112	0.2	0.937
Chongqing										
WMA-UA-SE	-47	0.057	10.8	0.01	1.33	<0.001	4.3	0.003	11.9	<0.001

Chongqing									
Model2									
2017	6	0.864	-0.3	0.965	-0.16	0.704	0.8	0.685	2.3	0.534
2018	31	0.388	-0.1	0.992	0.11	0.803	8.7	<0.001	5.2	0.168
2019	48	0.161	-3.6	0.53	-0.36	0.393	5.6	0.005	5.6	0.128
2020	11	0.748	-4.1	0.471	-0.52	0.216	5.9	0.003	4.5	0.221
2021	141	<0.001	3.3	0.567	-0.56	0.178	15.6	<0.001	7.8	0.034
2022	24	0.490	3.4	0.547	-0.29	0.494	7.9	<0.001	3.6	0.324
2023	78	0.023	3.7	0.513	-0.50	0.228	9.6	<0.001	5.4	0.143

UCA and 2016 were the control groups of mode1 and model2 respectively

Health risk assessment

In this study, AEDE, Ra_{eq}, ELCR and ADR were used to assess the hazards of radionuclides in soil of Chongqing in different years and regions, as shown in Table 8. Principal component analysis showed that PC1, PC2 and PC3 accounted for 70.06%, 17.64% and 6.78% of the total variance respectively. Cluster analysis divided all parameters into three clusters. Cluster I related to ^{40}K and ^{232}Th, cluster II composed of ^{226}Ra, ^{238}U, AEDE, Ra_{eq}, ELCR, ADR and cluster Ⅲ composed of ^{137}Cs, as shown in Figure 4. The results of cluster analysis were in good agreement with Spearman correlation analysis and PCA.

Table 8. Temporal and regional variation of radiological health risk

parameters in soil of Chongqing

Variables	AEDE(μSv.a^{-1})	Ra_{eq}(Bq•kg^{-1})	ELCR(10^{-3})	ADR（nGy•h^{-1}）
Years				
2016	76.40	132.66	0.30	62.29
2017	77.17	134.05	0.30	62.92
2018	84.48	147.59	0.33	68.88
2019	81.03	140.85	0.32	66.07
2020	79.10	137.99	0.31	64.50
2021	97.14	169.29	0.38	79.20
2022	85.55	149.45	0.33	69.75
2023	89.69	156.24	0.35	73.13
Regions				
UCA	80.78	140.39	0.32	65.87
UNA	88.44	154.63	0.35	72.11
TGRA-UA-NE Chongqing	81.59	141.13	0.32	66.53
WMA-UA-SE Chongqing	87.68	153.74	0.34	71.49
Arithmetic mean	84.03	146.39	0.33	68.52

The "Arithmetic mean" represented the average value of the health assessment for radioactive nuclides in soil across the entire study regions from 2016 to 2023.

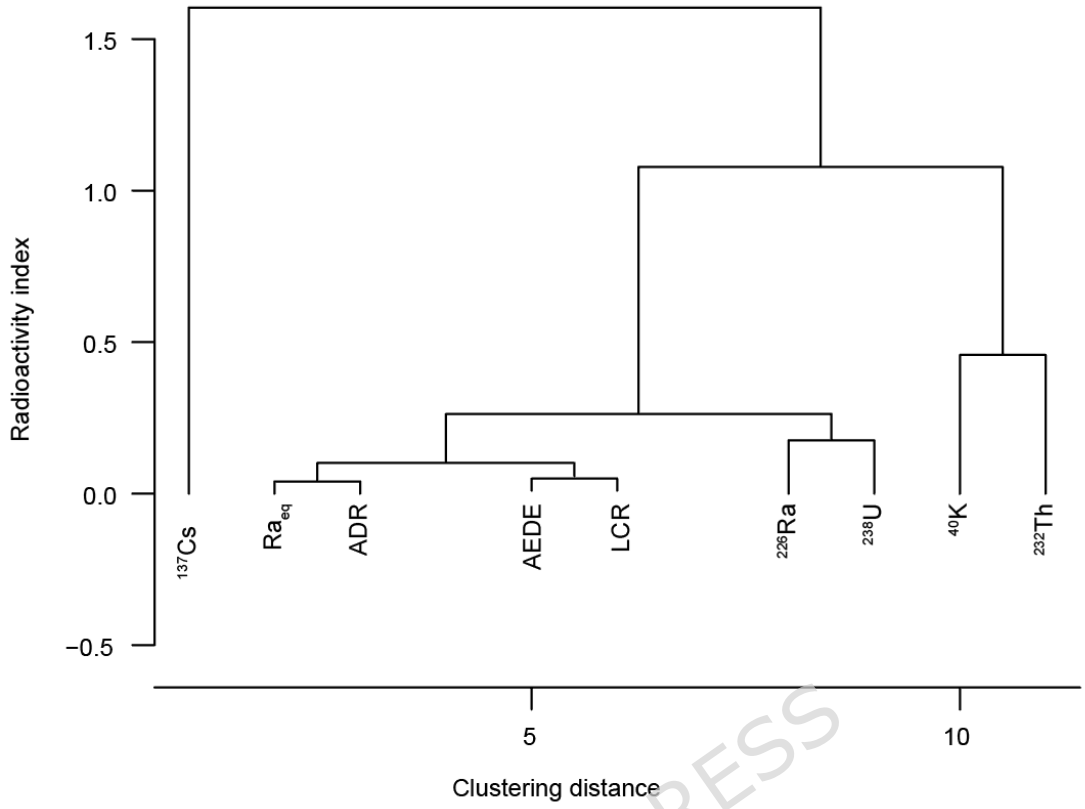

Figure 4. Cluster analysis of radionuclides in soil in Chongqing

Discussion

Natural radiation primarily originates from three purely natural sources: cosmic rays, cosmogenic radionuclides, and primordial radionuclides. An additional significant component arises from Technologically Enhanced Naturally Occurring Radioactive Materials (TENORM), where human activities have elevated the natural radiation levels[34]. Studies have found that natural background radiation is the primary source of radiation exposure to humans[35]. At the same time, soil plays an important role in the fate of natural radionuclides. Therefore, the study of radionuclides in the soil is a fundamental step in understanding the behavior of radioactivity in an ecosystem. these natural radionuclides emit radiation as they disintegrate, and this radiation contributes to the total absorbed dose for people (via ingestion, inhalation and external radiation)[36, 37]. Therefore, this study collected the monitoring data of natural radioactivity ^{40}K, ^{226}Ra, ^{232}Th and

^{238}U and artificial radionuclide ^{137}Cs in Chongqing soil from 2016 to 2023. Through descriptive analysis and fixed effect model analysis, the level of radionuclides in Chongqing soil was understood, and the regional and temporal differences of radionuclides in Chongqing soil were confirmed. Through health risks assessment, PCA and cluster analysis, the health effects of radionuclides in Chongqing soil were evaluated, and the relationship and classification of radionuclides were understood.

First of all, the measured concentrations of ^{40}K, ^{226}Ra, ^{232}Th and ^{238}U were found to be higher than the global median and population-weighted average. There is no relevant standard for the limit value of radionuclides in soil, and there is relatively little research on natural radionuclides in Chongqing, but relevant research in China shows that the typical background concentration range of ^{40}K is 140~850 (Bq/kg), ^{226}Ra, ^{232}Th and ^{238}U is 10~50 (Bq•kg^{-1})[38, 39]. Therefore, the relevant nuclides in soil of Chongqing were within the background concentration range of China. This study found that there was a positive correlation between ^{226}Ra and ^{232}Th, ^{238}U, which may be the result of the origin correlation of uranium series decay, the geochemical symbiosis of U-Th, and the superposition effect of regional geological environment[40, 41]. In addition, Chongqing is characterized by extensive mountainous and hilly terrain, where the erosion-deposition process on slopes causes soil particles rich in U, Th, and Ra to accumulate in low-lying areas, thereby further reinforcing the positive correlation among these three elements[38]. Meanwhile, three primary factors may explain the positive correlation observed between ^{40}K and ^{232}Th. Specifically, the homologous symbiosis of lithophile elements, synchronous enrichment throughout the entire pedogenic process, and the sorting effect of topographic and hydrological processes on nuclide distribution in Chongqing ' s mountainous, thereby further strengthening this positive correlation[42].

In our study, the results showed that there were significant differences in ^{40}K (F=6.272, P<0.001), ^{232}Th (F=24.390, P<0.001), ^{238}U (F=3.424, P=0.002<0.05) between different years, while there were no significant differences in ^{137}Cs and ^{226}Ra. The results may show that the radiation levels of ^{137}Cs and ^{226}Ra in Chongqing soil were relatively stable, and the time differences of ^{40}K, ^{232}Th and ^{238}U might be caused by artificial or natural factors, which needs to be further clarified in combination with more relevant data. The potential causes for the differential concentration variations of ^{238}U and ^{226}Ra in the soils of Chongqing are as follows: the redox sensitivity of ^{238}U and the strong adsorption capacity of ^{226}Ra form the innate basis for geochemical fractionation[43]. Natural processes including water level fluctuations in the Three Gorges Reservoir Area and mountain erosion serve as the dynamic regulatory drivers[44]. Anthropogenic disturbances such as agricultural fertilization and industrial activities act as the directional inducing factors for concentration shifts. In this study, Chongqing was divided into four regions. The results showed that ^{137}Cs (F=10.45, P=0.001<0.05), ^{232}Th (F=4.745, P=0.031<0.05) and ^{238}U (F=8.112, P=0.005<0.05) had statistically significant differences in the distribution of different regions, suggesting that there may be different baseline levels between different regions. Therefore, this study further used the fixed effect model for analysis and the results showed that after controlling the regional differences, the ^{40}K radiation level in soil in 2023 and 2021 were higher than that in 2016, the ^{232}Th radiation level in soil in 2018-2023 were higher than that in 2016, and the ^{238}U radiation level in soil in 2021 were higher than that in 2016. Those may be the result of the joint action of geological background (parent rock characteristics, tectonic activity), human activities (agricultural fertilization, energy development) and climatic processes (precipitation, weathering)[45]. Long-term anthropogenic activities, including industrial processes (particularly coal combustion and mining operations) and the continuous application of

phosphate fertilizers in agriculture, are the primary drivers of elevated radionuclide levels in regional soil systems[46]. Under the impact of the COVID-19 pandemic, the economy of Chongqing Municipality has experienced notable fluctuations since 2021[47]. This is highly likely to be a key factor contributing to the distinct concentration peaks of ^{40}K, ^{232}Th and ^{238}U observed in that year. After controlling the effects at different times, the activity concentrations of ^{226}Ra and ^{238}U in UNA were higher than those in UCA, and ^{226}Ra, ^{137}Cs, ^{232}Th and ^{238}U in WMA-UA-SE Chongqing were higher than those in UCA, respectively. Although the levels of radionuclides in the soils of Chongqing were within the safe range, the results implied that corresponding measures should be taken for different regions to monitor and manage different radionuclides.

The International Atomic Energy Agency and the International Commission on radiation protection recommend that the international general safety limit of Ra_{eq} should be less than 370 Bq/kg[48]. Ra_{eq} in the soil of Chongqing from 2016 to 2023 were in the normal range. This study found that the AEDE(84.03 $\mu Sv \cdot a^{-1}$), ELCR (0.33×10^{-3}) and ADR (68.52 $nGy \cdot h^{-1}$) of radionuclides in soil of Chongqing were higher than the global outdoor AEDE average value of 70 $\mu Sv \cdot a^{-1}$, the average level of ELCR (0.29×10^{-3}) and the global typical background range average value of ADR (60 $nGy \cdot h^{-1}$)[48]. This result is consistent with the AEDE value (81.83 $\mu Sv \cdot a^{-1}$) of sediments in the Yangtze River Estuary in the literature[49]. The ADR and AEDE of radioactive nuclides in Chongqing soil are higher than the ADR (55 $nGy \cdot h^{-1}$) and calculated AEDE (67.45 $\mu Sv \cdot a^{-1}$) of natural radiation (land gamma external irradiation) in the UNSCEAR 2008 report[19]. In this study, all parameters were also divided into three clusters. Cluster I related to ^{40}K and ^{232} Th. Cluster Ⅱ composed of ^{226}Ra, ^{238}U , and cluster Ⅲ composed of ^{137}Cs. These results implied that the co-association of ^{40}K and ^{232}Th suggests a common geogenic origin, as both are typically found together in igneous rocks and

other bedrock formations[42]. The association of ^{226}Ra and ^{238}U underscores their geochemical coherence, as both radionuclides belong to the uranium decay series and are typically found together in specific geological settings like phosphate-rich deposits and granitic rocks[50]. Conversely, ^{137}Cs was distinctly segregated into Cluster III, consistent with its purely anthropogenic origin from global fallout and nuclear accidents, which distinguishes it from naturally occurring radionuclides. Although ^{40}K and ^{137}Cs share certain chemical similarities, they were not grouped into the same category in this cluster analysis. This likely reflects their fundamentally different origins and environmental behaviors: ^{40}K is a ubiquitous natural radionuclide whose distribution is primarily controlled by the regional geochemical background[51]. Whereas ^{137}Cs is an anthropogenic fission product whose spatial distribution is strongly influenced by the local heterogeneity of historical atmospheric deposition events and its unique adsorption and migration behavior in soil[52]. Consequently, despite their chemical affinity, their distinct origins and subsequent environmental processes govern the differences in their spatial distribution patterns within the current study area[53].

This comprehensive dataset offered the first multi-year, region-wide characterization of soil radionuclides in Chongqing, serving as a critical reference for environmental protection and public health governance. Based on the results of soil monitoring in Chongqing from 2016 to 2023, this study identified the temporal and regional differences of radionuclides in soil of Chongqing for the first time. By calculating various health risk indicators, this study focused on evaluating the health risk of radionuclides in soil to residents in Chongqing. However, there are still some shortcomings in this study. Firstly, there was no way to directly assess the internal exposure caused by soil. Further, the living environment and conditions of different residents are different. Rural residents have a greater chance and longer

time to contact with soil than urban residents, and the health risk of radionuclides in soil is also greater, but this study can not assess the health risk of different residents or individual residents. Therefore, the internal exposure pathways (ingestion and inhalation) should be assessed in future work. While this study has identified statistically significant spatial differences in the levels of certain radionuclides across Chongqing, the underlying drivers for these variations (e.g., specific industrial activities, detailed geological substrate differences, or agricultural practices) remain unclear based on the current data. Therefore, it would be premature to propose specific regulatory measures for individual regions. Instead, these findings serve as a crucial foundation and clearly define the direction for future research.

Conclusion

Although the concentrations of radionuclides detected in the soil of Chongqing were all within the scope of relevant safety thresholds, the overall levels were consistently higher than the typical global baseline conditions. In particular, the specific activities of the natural radionuclides ^{40}K, ^{232}Th, and ^{238}U presented distinct annual fluctuations throughout the monitoring period, which underscores the necessity of further strengthening long-term, systematic monitoring of soil radionuclide dynamics in this region. With regard to regulatory supervision, it is suggested that the UNA prioritize the enhancement of surveillance efforts targeting ^{226}Ra and ^{238}U. Meanwhile, the WMA-UA-SE Chongqing is advised to expand regulatory oversight to include a broader spectrum of radionuclides, encompassing ^{226}Ra, ^{137}Cs, ^{232}Th, and ^{238}U, particularly the anthropogenic radionuclide ^{137}Cs as an indicator of fallout-related contamination. Results of the health risk assessment demonstrated that AEDE, ELCR, and ADR associated with soil radionuclides in Chongqing all exceeded the global average levels. While these elevated values do not constitute an immediate health hazard or trigger an urgent

alarm, they clearly indicate that the soil radionuclide background in Chongqing is higher than the typical global baseline conditions.

In conclusion, to comprehensively clarify the long-term variation trends of soil radionuclide levels in Chongqing and their potential environmental and health implications, it is imperative to carry out in-depth follow-up research and establish a standardized, high-resolution baseline dataset for soil radionuclides in this region.

Acknowledgements

We would like to thank all staff who collected and detected samples and recorded and managed the data in the Chongqing Radiation Environment Supervision and Management Station, as well as all staff of subordinate institutions who provided assistance in this study.

Author contributions

Qiang Huang and Xue Zhao cleaned and analyzed the data and wrote the initial draft. Jun Diao made significant contributions to conceive the study, revised the manuscript and submitted. Hengyan Du, Bo Fang, Qiang Tan, Qiuhao Zhang, Li Chen and Cuilan Fang reviewed the draft and provided critical suggestions, which helped improve the manuscript. All authors reviewed the manuscript and agreed on the final version of the manuscript to be submitted for publication.

Data availability statement

The data that support the findings of this study are openly available from Annual Report of Chongqing's Radiation Environment. Data are located in controlled access data storage at Chongqing Radiation Environment Supervision and Management Station, Chongqing, China. The data

supporting the findings of this study are available from the corresponding author upon reasonable request.

Funding

This research was supported by the Chongqing Science and Health Joint medical research Project (No. 2025MSXM056). This research was also supported by the Chongqing Center for Disease Control, Prevention and Chongqing Jiulongpo District Center for Disease Control and Prevention, Chongqing Radiation Environment Supervision and Management Station and Chongqing Medical University.

Declarations

Competing interests

The authors declare no competing interests.

References

1. Mbonu, C.C. et al. Assessment of terrestrial radionuclide exposure and contamination rates within the Mbaitoli area, Nigeria. *Sci Rep* **15**, 28702 (2025).
2. Nhon, D.H. et al. Radioactive concentrations and natural radionuclide risks in Ha Long Bay and Ba Che Estuary sediments, Vietnam. *Environ Monit Assess* **197**, 695 (2025).
3. Erzin, S. et al. Natural radioactivity levels and related risk assessment in soil and rock samples from the Çine submassif, defining Western Anatolia, Turkey. *Environ Monit Assess* **197**, 919 (2025).
4. Hasan, S., Iasir, A.R.M., Ghosh, T.K., Sen Gupta, B. & Prelas, M.A. Characterization and Adsorption Behavior of Strontium from Aqueous Solutions onto Chitosan-Fuller's Earth Beads. *Healthcare (Basel)* **7** (2019).
5. Kato, T., Yamada, K. & Hongyo, T. Area Dose-Response and Radiation Origin of Childhood Thyroid Cancer in Fukushima Based on Thyroid Dose in UNSCEAR 2020/2021: High 131I Exposure Comparable to Chernobyl. *Cancers (Basel)* **15** (2023).
6. Su, J. et al. Monte Carlo calculation of artificial radionuclide radiation dose rates for marine species in the Western Pacific. *Radiat Prot Dosimetry* **158**, 479-486 (2014).

7. Zhong, N., Li, L., Yang, X. & Zhao, Y. Analytical Methods for the Determination of (90)Sr and (239,240)Pu in Environmental Samples. *Molecules* **27** (2022).
8. Machraoui, S., Labidi, S. & Purushotham, M.M. Assessment of gamma absorbed doses and radiological risk indexes from soil radioactivity around the phosphate area in south Tunisia. *Radiat Prot Dosimetry* **200**, 387-395 (2024).
9. Maglas, N.N.M. et al. Natural radioactivity level in Yemen: A systematic review of radiological studies. *Appl Radiat Isot* **210**, 111343 (2024).
10. Ahmad, A.Y., Al-Ghouti, M.A., AlSadig, I. & Abu-Dieyeh, M. Vertical distribution and radiological risk assessment of 137Cs and natural radionuclides in soil samples. *Sci Rep* **9**, 12196 (2019).
11. Li, P. et al. Radiocesium distribution caused by tillage inversion affects the soil-to-crop transfer factor and translocation in agroecosystems. *Sci Total Environ* **831**, 154897 (2022).
12. Elizabeth, D.E., Janice, W., Nicholas, I.J. & Joyce, P. External radiation exposure and mortality in a cohort of uranium processing workers. *American Journal of Epidemiology*, 91-95 (2000).
13. Darby, S. et al. Radon in homes and risk of lung cancer: collaborative analysis of individual data from 13 European case-control studies. *Bmj* **330**, 223 (2005).
14. Rashid, N.S.A. et al. Assessment of Uranium and Thorium Co-contaminant Exposure from Incidental Concrete Dust Ingestion. *Korean Journal of Chemical Engineering* **41**, 10 (2024).
15. Sartayev, Y. et al. Internal radiation exposure from 137Cs and its association with the dietary habits of residents from areas affected by the Chernobyl nuclear accident, Ukraine: 2016-2018. *PLoS One* **18**, e0291498 (2023).
16. (IEA, 2023).
17. Aközcan Pehlivanoğlu, S., Mancini, S., Özden, S., Guida, M. & Falanga, M. Characterization of a typical urban soil in terms of natural radionuclide content. The case study of a university campus. *Heliyon* **10**, e37145 (2024).
18. Oladejo, O.F., Olukotun, S.F., Rufai, A.B. & Mathuthu, M. Assessment of radiation hazards from natural radionuclide activity in quarry sites and surrounding soils in Osun State, Southwest Nigeria. *Sci Rep* **15**, 19345 (2025).
19. United Nations Scientific Committee on the Effects of Atomic Radiation (UNSCEAR). *Sources and Effects of Ionizing Radiation: UNSCEAR 2008 Report to the General Assembly with Scientific Annexes* (United Nations, New York, 2010).
20. Lasheen, E.S.R. et al. Radiological Hazards and Natural Radionuclide Distribution in Granitic Rocks of Homrit Waggat Area, Central Eastern Desert, Egypt. *Materials (Basel)* **15** (2022).

21. Salman, A.Y., Kadhim, S.A., Hussain, H.M. & Sharrad, F.I. Assessing the Excess Lifetime Cancer Risk from Water in the Euphrates River, Najaf, Iraq. *Health Phys* (2025).
22. Shapiro, B. 1990 Recommendations of the International Commission on Radiological Protection: ICRP Publication 60, Pergamon Press, 1991. *European Journal of Radiology* **15**, 93 (1992).
23. Renborg, L. et al. Rapid decline of cerebrospinal fluid biomarkers of axonal injury and neuroinflammation after initiation of antiretroviral therapy in HIV. *J Neurovirol* (2025).
24. Tang, F., Zhu, Y., Jayawardena, D., Jin, G. & Jiang, Y. Sleep quality and cognitive functioning among Chinese older adults living in the US: a mixed-effects model analysis. *BMC Geriatr* **25**, 52 (2025).
25. Faheem, M., Mujahid, S.A. & Matiullah Assessment of radiological hazards due to the natural radioactivity in soil and building material samples collected from six districts of the Punjab province-Pakistan. *Radiation Measurements* **43**, 1443-1447 (2008).
26. Hamzah, Z., Rahman, S.A.A., Saat, A. & Hamzah, M.S. EVALUATION OF NATURAL RADIOACTIVITY IN SOIL IN DISTRICT OF KUALA KRAI, KELANTAN. *Malaysian Journal of Analytical ences* **16**, 335 (2012).
27. Turhan, S.K., A.Varinlioglu, A.Sahin, N. K.Arkan, I.Oguz, F.Yucel, B.Ozdemir, T. Distribution of terrestrial and anthropogenic radionuclides in Turkish surface soil samples. *Geoderma: An International Journal of Soil Science* **187/188** (2012).
28. Rafique, M. & Jabbar..., A. Radiometric analysis of rock and soil samples of Leepa Valley; Azad Kashmir, Pakistan. *Journal of Radioanalytical & Nuclear Chemistry* **298**, 2049-2056 (2013).
29. Sharma, R.L. et al. Natural Radioactivity, Radon Exhalation Rates and Radiation Doses in the Soil Samples Collected from the Vicinity of Kolaghat Thermal Power Plant, West Bengal, India. *Indian Journal of Pure & Applied Physics* **61** (2023).
30. Kürküolu, M.E., Kahraman, F.A., Dizman, S. & Cengiz, G.B. Evaluation of radioactivity and radiological parameters in soil samples in Isparta, Türkiye. *Nuclear Engineering and Technology* (2024).
31. Muhammad, A.N., Ismail, A.F. & Garba, N.N. Natural radioactivity in food crops and soil and estimation of the concomitant dose from tin mining areas in Nigeria. *Journal of Taibah University for Science* **18**, Article: 2366507 (2024).
32. Maglas, N.N.M. et al. Natural radioactivity level in Yemen: A systematic review of radiological studies. *Applied radiation and isotopes : including data, instrumentation and methods for use in agriculture, industry and medicine* **210**, 111343 (2024).
33. Machraoui, S., Labidi, S. & Purushotham, M.M. Assessment of gamma absorbed doses and radiological risk indexes from soil radioactivity around the phosphate area in south Tunisia. *Radiat Prot Dosimetry*

(2024).

34. Natarajan, T. et al. Natural radionuclides and radiological risk assessment in the stream and river sediments of a high background natural radiation area Kanyakumari, India. *Environ Monit Assess* **196**, 330 (2024).
35. Jain, V. et al. Non-linear dose response of DNA double strand breaks in response to chronic low dose radiation in individuals from high level natural radiation areas of Kerala coast. *Genes Environ* **45**, 16 (2023).
36. Yang, B. et al. Dietary exposure of radionuclides and heavy metals in adult residents in a high background natural radiation area using duplicate diet method. *Sci Rep* **12**, 16676 (2022).
37. Liu, C., Benotto, M., Ungar, K. & Chen, J. Environmental monitoring and external exposure to natural radiation in Canada. *J Environ Radioact* **243**, 106811 (2022).
38. Khan, I.U., Sun, W. & Lewis, E. Review of low-level background radioactivity studies conducted from 2000 to date in people Republic of China. *Journal of Radiation Research and Applied Sciences* **13**, 406-415 (2020).
39. Song, G., Chen, D., Tang, Z., Zhang, Z. & Xie, W. Natural radioactivity levels in topsoil from the Pearl River Delta Zone, Guangdong, China. *J Environ Radioact* **103**, 48-53 (2012).
40. Tan, S. et al. Output characteristics and driving factors of non-point source nitrogen (N) and phosphorus (P) in the Three Gorges reservoir area (TGRA) based on migration process: 1995–2020. *Science of The Total Environment* **875**, 162543 (2023).
41. Teku, D. & Workie, M.D. Longitudinal analysis of soil erosion dynamics using the RUSLE model in Ethiopia's Lake Ziway watershed: implications for agricultural sustainability and food security. *Frontiers in Environmental Science* **Volume 12 - 2024** (2025).
42. Lovrenčić Mikelić, I., Oreščanin, V. & Barišić, D. 40K, 226Ra, 232Th, 238U and 137Cs relationships and behaviour in sedimentary rocks and sediments of a karstic coastal area (Kaštela Bay, Croatia) and related rocks and sediments' differentiation. *Environ Sci Pollut Res Int* **28**, 51497-51510 (2021).
43. Rodriguez, V.G. et al. Radiological Analyses of 226Ra and 238U in Surface Water and Sediments from the Jackpile Member of the Morrison Formation, Pueblo of Laguna, New Mexico. *Environ Sci Technol* (2024).
44. Dinh, M.A. et al. Concentration and distribution characteristics of gross alpha, 238U, 234U and 226Ra in freshwater of some rivers and artificial lakes in southeast Vietnam. *Appl Radiat Isot* **225**, 112064 (2025).
45. Bellotti, E., Broggini, C., Di Carlo, G., Laubenstein, M. & Menegazzo, R. Search for time modulations in the decay constant of 40K and 226Ra at the underground Gran Sasso Laboratory. *Physics Letters B* **780**, 61-65 (2018).
46. Popoola, O.J., Olubi, O.E., Bamidele, S.E. & Adepoju, A.O. Geochemical

distribution, pollution evaluation, and radiological health hazards of naturally occurring radionuclides in soil and stream sediments from Idanre area, Southwest Nigeria. *Discover Geoscience* **3**, 169 (2025).

47. Zhang, J. & Li, H. The Impact of Big Data Management Capabilities on the Performance of Manufacturing Firms in Asian Economy During COVID-19: The Mediating Role of Organizational Agility and Moderating Role of Information Technology Capability. *Front Psychol* **13**, 833026 (2022).
48. Paquet, F. et al. ICRP Publication 137: Occupational Intakes of Radionuclides: Part 3. *Ann ICRP* **46**, 1-486 (2017).
49. Wang et al. Natural radioactivity assessment of surface sediments in the Yangtze Estuary. *Marine Pollution Bulletin* (2000).
50. Ilori, A.O. & Chetty, N. A review of the occurrence of naturally occurring radioactive materials and radiological risk assessment in South African soils. *Int J Environ Health Res* **34**, 2969-2982 (2024).
51. Ghias, S. et al. Assessment of the radiological doses and health risk from natural and anthropogenic radionuclides in wheat samples near nuclear facilities in Dera Ghazi Khan. *Journal of Radioanalytical and Nuclear Chemistry* **334**, 1497-1507 (2025).
52. Du, P. & Walling, D.E. Using 137 Cs measurements to investigate the influence of erosion and soil redistribution on soil properties. *Appl Radiat Isot* **69**, 717-726 (2011).
53. Huang, C. et al. Environmental correlates of the distribution characteristics of artificial radionuclides (137Cs, 239+240Pu, 237Np) in the northeast China. *J Hazard Mater* **490**, 137759 (2025).